LIGO: Status and Recent Results

Raymond E. Frey *for the LIGO Scientific Collaboration*

Department of Physics, University of Oregon, Eugene, OR 97403

Abstract. An overview of LIGO is given. The detectors have reached design sensitivity and a long science run (S5) is currently in progress. A snapshot is given of some recent results prior to S5. No detections of gravitational radiation can be reported. Prospects for S5 and beyond are provided.

Keywords: gravitational waves
PACS: 04.80.Nn, 95.55.Ym, 07.60.Ly

LIGO DETECTORS

The Laser Interferometer Gravitational Wave Observatory (LIGO) consists of three long-baseline interferomters on two sites, one at the Hanford Reservation near Richland, Washington and the other about 40 km east of Baton Rouge, Louisiana. Each instrument is a Michelson interferometer with arms which are Fabry-Perot cavities. At the Hanford site (LHO) two interferometers share the vacuum enclosure, one with 4 km arms (H1) and one with 2 km arms (H2). At the Livingston site (LLO) there is a single 4 km interferometer (L1). The LIGO Laboratory, managed by Caltech and MIT, was responsible for the design and construction of the LHO and LLO facilities, as well as their current operations. Research associated with gravitational wave science is carried out by the LIGO Scientific Collaboration (LSC), consisting of scientists from about 50 universities and institutions worldwide, including members from the LIGO Caltech and MIT groups, and from the GEO600 collaboration.

The design of the initial LIGO instruments[1] was based on reaching sufficient sensitivity to detect gravitational wave radiation from the last ∼minute of a coalescing binary neutron star system at the distance of the Virgo cluster of galaxies. Gravitational wave emission requires a time varying mass quadrupole moment. A binary system consisting of compact objects, typically neutron stars or black holes, represents an efficient radiator, with $\sim 1\%$ of the system rest energy appearing as gravitational radiation. The framework[2] for calculations within General Relativity is well established. Recent advances in numerical relativity[3] have allowed calculations of binary systems to be extended from the post-Newtonian regime (approaching the last stable orbit) to the strong gravity regime near merger. An approximate form of the quadrupole formalism provides an estimate for the required detector sensitivity:

$$h \sim \left(\frac{GM}{c^2}\right)\left(\frac{v^2}{c^2}\right)\frac{1}{r} \tag{1}$$

Here, h is the gravitational-wave (GW) strain – the stretching of the local spacetime, $h = \delta L/L$; M is the mass which is moving at speed v. The strain h is analogous to the

electromagnetic radiation fields, which also fall with (large) distance from a source as $1/r$. For one solar mass, $M = M_\odot$, and $v \approx c$, then at $r = 15$ Mpc (Virgo cluster) this gives $h \sim 3 \times 10^{-21}$. Hence, even for an $L = 4$ km interferometer this represents a required length sensitivity of $\sim 10^{-18}$ m.

The Fabry-Perot cavities are formed by suspended optics at each end of the interferometer arms. The resonant swing frequency of the suspended optics is about 1 Hz. Hence, for motion along the arms at frequencies well above 1 Hz, the suspended optics represent inertial, "freely falling" test masses. The optical phase shift due to a length change $\delta L = hL$ for one round trip by the light in an interferometer arm is $\delta\phi = 4\pi Lh/\lambda$, where the laser wavelength λ is 1.064 μm. The light in the arm cavities undergoes about 100 bounces, which increases the phase shift by this factor. Hence, a required strain sensitivity of 10^{-21} corresponds to a phase shift of 10^{-9} rad, which is about two orders of magnitude better than typical lab interferometers. A number of technical innovations[4] make this possible. The control of this sensitive instrument involves many intertwined servo systems. A high-gain servo system controls the position of the test masses so that a readout photodiode at one of the two interferometer output ports is centered on an interference minimum (the "dark port"). The "GW channel," used in GW searches, is derived from the error signal for this servo system.

To calibrate the GW channel, known electronic signals are injected into the control system, thereby inducing test mass motions of known amplitude. The output GW channel is thus calibrated in terms of the physical strain $\delta L/L$. The same system is used to inject astrophysically motivated GW waveforms, so that the full hardware and software chains can be exercised as for real gravitational waves. These are referred to as "hardware injections" by the analysis groups.

Figure 1 gives the LIGO sensitivity in the form of the power spectral density of the noise in the GW channel. It is calibrated in terms of strain as mentioned above, hence the noise spectrum has units of GW strain per $\sqrt{\text{Hz}}$. Table 1 gives the basic information for the five LIGO science runs to date. Figure 1 clearly indicates the significant improvements in sensitvity since the S1 run. The curve marked "LIGO I SRD Goal" is from the initial LIGO design. The sensitivity for the S5 run has approximately achieved this goal – worse than design below ≈ 70 Hz and better than design at high frequency. The figure shows the LHO H1 sensitivity for S5. The L1 sensitivity for S5 is similar to H1, while the 2 km H2 interferometer is about half as sensitive, as expected.

The overall shape of the noise curves in Fig. 1 is dominated by seismic noise at low frequency and shot noise for frequencies above 200 Hz. Shot noise is mitigated by maintaining a high optical power level. In addition to the light storage in the arm cavities, a power recycling mirror redirects exiting light back into the interferometer. This provides an additional factor of ≈ 30, so that a few Watts of input laser power results in a few kW of power in the arms. Since the average light storage time is about 1 ms, the sensitivity decreases at higher GW frequency, as the stored light is increasingly sensitive to the full GW phase, *i.e.* both signs of δL. In the 40-100 Hz range, upconversion of seismic noise is currently (S5) limiting the sensitivity. A number of narrow lines can be seen above the noise floor. The most prominent are due to AC power pick up (60 Hz and harmonics) and the suspension wire resonances (fundamentals at about 345 Hz and harmonics), also known as violin modes. In addition there are three calibration lines, as discussed above, which are always present in science run data.

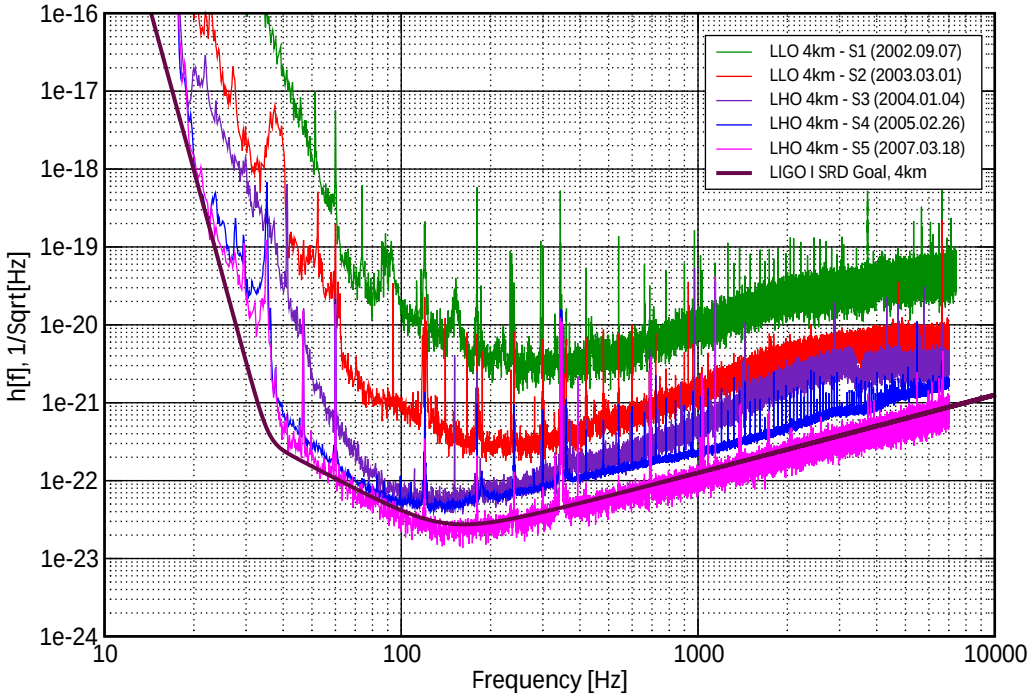

FIGURE 1. LIGO instrumental sensitivity for science runs S1 (2002) to S5 (present) in units of gravitational-wave strain per square root Hz as a function of frequency.

In addition to the main GW channel, hundreds of other data channels are recorded in the primary data records, known as frames. These include the output of monitors of the local environment, such as seismic activity, other locally-induced ground motion, acoustic signals, electromagnetic fields or signals, and weather information. Controlled injections of environmental signals are regularly performed to determine or monitor the various couplings to the interferometer. Unusual or transient behavior in these environmental channels is identified and used to set data quality flags, which depending on their severity, can be used to inform or even veto a segment of data used in an astrophysical GW search analysis.

TABLE 1. LIGO science runs. The completion of run S5 is expected in fall 2007.

S1	9/2002 (17 days)
S2	2/2003 – 4/2003 (59 days)
S3	11/2003 – 1/2004 (70 days)
S4	2/2005 – 3/2005 (30)
S5	11/2005 – Fall 2007 ($\sim$ 700 days)

The goal of initial LIGO is to collect one year of data at design sensitivity. This is the S5 science run. The one year has been interpreted as a year of coincidence data between the LHO and LLO interferometers, which will take nearly two calendar years

to complete, due to the imperfect up time of the interferometers. A few of the important contributors to down time are anthropogenic seismic noise, especially logging, at LLO, and high winds, which induce seismic noise, at LHO.

GRAVITATIONAL WAVE SEARCHES

Gravitational waves in General Relativity propagate at speed c in two independent polarization states, denoted by $+$ (plus) and $\times$ (cross). If we imagine an incident gravitational wave propagating in the z-direction with $+$ polarization which stretches (shrinks) the local spacetime in the x- (y-) direction, then a $\times$ polarized wave has the same effect on a ccordinate system rotated by 45°. In general, the response of an interferometer to a gravitational wave $(h_+, h_\times)$ from a location (θ, ϕ) in the sky is given by

$$h(t) = F_+(\theta, \phi, \psi)\, h_+(t) + F_\times(\theta, \phi, \psi)\, h_\times(t) \tag{2}$$

where ψ represents the orientation of the GW polarization. The functions F_+ and $F_\times$ are often referred to as interferometer antenna functions.

Gravitational wave searches in LIGO are conveniently divided into four categories by astrophysical source type (and analysis technique). These correspond to the four major analysis groups in the LSC. In the following sections, a few highlights from recent publications and prospects for the S5 run are presented for each category.

Compact Binary Sources

As mentioned above, the final inspiral just before the merger of a compact binary system – binary neutron star (BNS), binary black hole (BBH), or neutron star-black hole (NSBH) – represents an efficient GW radiator, and one which is theoretically well modeled. Because of the latter property, the interferometer data can be filtered through a bank of template functions, each of which describes a possible GW waveform from an inspiral. These waveforms have the general form

$$h(t) = \frac{1\ \mathrm{Mpc}}{D_{\mathrm{eff}}} A(t) \cos(\phi(t) - \phi_0) \tag{3}$$

where $A(t)$ and $\phi(t)$ depend on the masses and spins of the binary system objects. D_{eff} corresponds to the physical distance D when it is optimally oriented in the sky with respect to the interferometer (optimal antenna pattern) and when the radiation pattern from the source is optimal (when the orbital plane of the binary system is perpendicular to the line of sight to earth). On average (averaged over orientation and sky position), $D_{\mathrm{eff}}/D = 2.3$. When the spins are not large, the inspiral waveform is sinusoidal with amplitude and frequency (twice the orbital frequency) which increase until the innermost stable circular orbit (ISCO), after which the objects plunge toward coalescence.

In the inspiral analysis[5] of the S3 and S4 run data, three distinct searches are performed, separated by the mass ranges of the target binary systems: Primordial black hole binary (PBH) systems where each mass is between 0.3 and 1.0 solar masses; binary

neutron star (BNS) systems where each mass is between 1.0 and 3.0 solar masses; and stellar mass black hole binary (BBH) systems with component masses between 3.0 and 40 (S3) or 80 (S4) solar masses. The masses determine the frequency range and the duration of the GW signal within the sensitive LIGO band (see Fig. 1). Whereas the BNS search uses templates which take up to 44 s to pass through the LIGO band, the BBH duration is only a few seconds, since the last orbit is at a relatively low frequency ($f_{\rm ISCO} \sim 4\ {\rm kHz}/(M/M_\odot)$).

No inspiral events have been observed through the S4 run. Figure 2 gives the LIGO limits combined from the S3 and S4 runs. The rate is in units of number per year per L_{10}, where L_{10} is 10^{10} times the blue solar luminosity. The Milky Way represents $1.6L_{10}$. For the PBH amd BNS searches, the limits improve with mass since the signals are larger and the searches are therefore deeper. In the BBH case, the larger masses have a smaller ISCO frequency and hence a measurable signal of shorter duration. This can be seen in the right-hand panel of Fig. 2 for total mass greater than about $40M_\odot$.

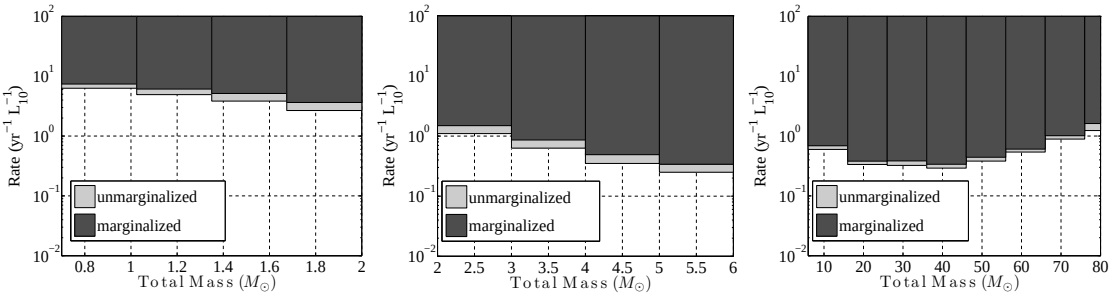

FIGURE 2. Limits from the LIGO S3 and S4 runs on the rate of primordial BBH (left), BNS (middle), and BBH (right) coalescences as a function of the total mass of the system in units of solar masses. The shaded regions are excluded – the lighter shaded region includes only statistical errors, while the darker shading includes systematic errors.

The improved sensitivity for the S5 run means that for the BNS search, about 200 Milky Way equivalent galaxies (MWEGs) are in range of the search. For the BBH search (each mass $5M_\odot$) about 1000 MWEGs are in range.

Stochastic Sources

A large number of unresolved sources, either of cosmological or astrophysical origin, would give rise to a background of gravitational waves. For example, inflationary cosmologies predict such a cosmic GW background, albeit at rather a low level relative to the LIGO sensitivity (see Fig. 3). Sufficiently large stochastic signals would be detectable by the H1-L1 or H2-L1 LIGO interferometers as a correlated signal underlying uncorrelated detector noise. A cross-correlation statistic Y is formed for an interferometer pair from the product of the (Fourier-transformed) times series of each, folded with an optimal filter function, and summed over frequency. Both Y and its variance are sensitive to the spectrum of GW energy density,

$$\Omega_{GW} = \frac{f}{\rho_c}\,\frac{d\rho_{GW}}{df} \tag{4}$$

where $\frac{d\rho_{GW}}{df}$ is the GW energy density spectrum and ρ_c is the cosmological critical density. In practice, a parameterization of the form $\Omega_{GW} = \Omega_\alpha \, (f/100 \text{ Hz})^\alpha$ is used.

The most recent LIGO result[6], from science run S4, is a limit on the GW energy density which is starting to be competitive with other limits and of interest for confronting some models. For $\alpha = 0$, the 90% upper limit from S4 is

$$\Omega_{GW} < 6.5 \times 10^{-5} \tag{5}$$

This is the current best limit in the LIGO band (50-150 Hz). Figure 3 shows the S4 result, along with the expected sensitivity from the LIGO S5 run and from Advanced LIGO. A number of representative model expectations are shown in the figure, as well as other limits. See [6] for the details. It is noteworthy that the LIGO sensitivity following S5 will surpass the BBN limit, where the formation of light nuclei is sensitive to the GW energy density.

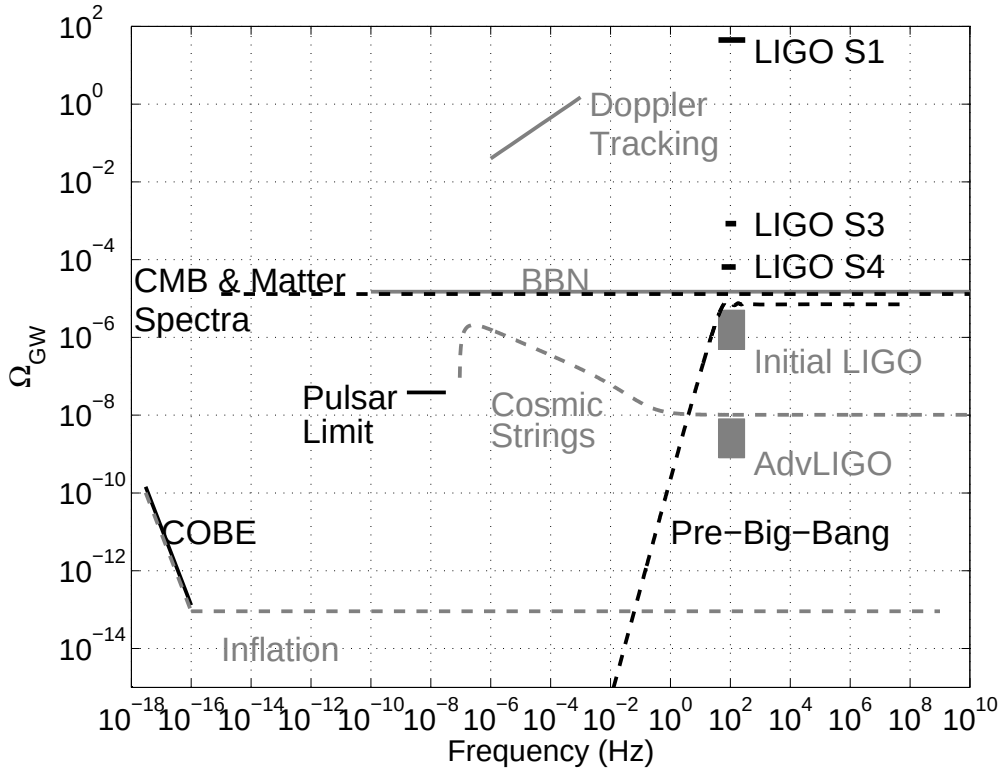

FIGURE 3. Experimental constraints and representative theoretical expectations, as discussed in [6], for the stochastic gravitational wave energy density as a function of frequency. The current best LIGO limit and expectations for S5 (Initial LIGO) and Advanced LIGO (AdvLIGO) are indicated near 100 Hz.

Periodic Sources

These searches are for GW emission from pulsars, either by targeting known pulsars or all-sky searches of unknown periodic GW radiators. A pulsar can only emit gravi-

tational radiation if there is an asymmetry in the mass distribution with respect to the rotation axis. Such asymmetries can naturally arise from several mechanisms and the expected dominant GW emission is at twice the rotation frequency. Young pulsars, such as the Crab pulsar (PSR J0534+2200), are seen as especially good candidates, and in fact are observed to have frequent strong glitches in their electromagnetic signals, perhaps an indication of asymmetries. A pulsar at distance r has a GW strain amplitude (assuming optimal orientation) of

$$h_o = \frac{16\pi^2 G}{c^4}\,\frac{\varepsilon I_{zz}\nu^2}{r} \tag{6}$$

where ν is the spin frequency, I_{zz} is the dominant principal moment of inertia and $\varepsilon = (I_{xx} - I_{yy})/I_{zz}$ is the equatorial ellipticity. If one supposes that a pulsar's decrease in spin frequency is due to the emission of gravitational radiation, that is $dE/dt = 4\pi^2 I_{zz}\nu\dot{\nu}$ is equal to the GW power, then one can find the corresponding GW strain amplitude, known as the spin-down limit, $h_{\rm sd}$. Observationally approaching this limit is seen as an indication of astrophysical relevance.

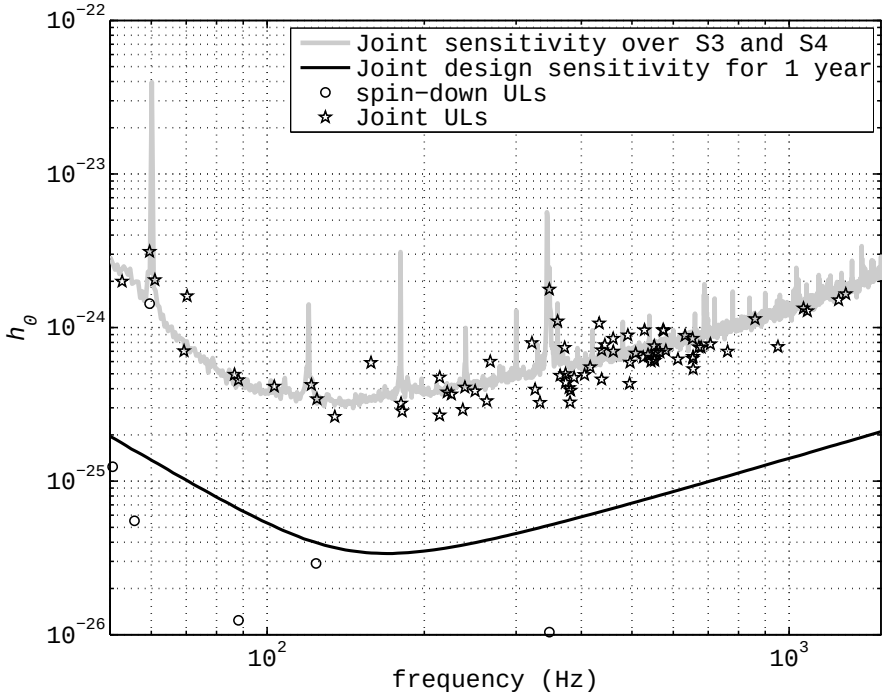

FIGURE 4. Upper limits (stars) on GW emission from 78 known pulsars in the S3 and S4 data. These limits closely follow the calculated joint sensitivity curve for S3 and S4. The corresponding sensitivity curve for a year of data at design sensitivity is also given.

The combined S3 and S4 data were used to provide direct GW searches of 78 known pulsars[7]. The search employs a heterodyne technique, and the phase model for each pulsar is updated using the radio or X-ray data. Only pulsars with good timing data are retained. The data was coherently combined over the S3 and S4 runs. The GEO600 detector, which had comparable sensitivity to LIGO during this running period for

frequencies above about 1 kHz, was also used for the highest frequency pulsars. No evidence for a GW signal was found. Figure 4 summarizes the 95% CL upper limits.

Figure 4 also indicates the spin-down limit $h_{\rm sd}$ mentioned above for some pulsars. Most notably, $h_{\rm sd}$ for the Crab pulsar (near 60 Hz) is within a factor of 2.2 of the S3-S4 result. It is clear from the figure, that the S5 run will surpass this limit. In addition the S5 data will provide upper limits on GW strain and ellipticity ε for some pulsars (assuming no GW detection) of $\sim 1\times 10^{-25}$ and $\sim 1\times 10^{-7}$, respectively.

GW Burst Searches

A GW "burst" is considered to be a gravitational waveform which is unmodeled. Typically, the burst techniques focus on searches for short-duration ($\ll 1$ s) GW signals, for example due to core-collapse supernovae or the merger phase of a compact binary inspiral. Bursts searches include an all-sky search over all science run data and searches made in association with an independent astrophysical signature ("triggered" searches), such as a gamma-ray burst or SGR detection. An example result from each of these is given below.

All-sky Search

The data from each interferometer is initially analyzed using the WaveBurst algorithm, which performs a linear wavelet packet decomposition, producing a time-frequency map of each short data interval. Time-frequency pixels which contain excess signal power are examined and combined with significant pixels in the other interferometers to form clusters, the most significant of which form a set of triggers. Two types of signal consistency checks between triggers from each interferometer are performed, data-quality conditions are applied, and for the surviving triggers time-shifted data (background) is compared to the zero time lag foreground to evaluate significance.

No significant excess has been observed. The results[8] giving exclusion curves in the trigger rate versus GW strain from the S4 run (and compared to S1 and S2) are given in Fig. 5. In order to consider a wide variety of possible signal waveforms, the results are expressed in terms of the quantity $h_{\rm rss}$, which is related to a detected GW waveform $h(t)$ by

$$h_{\rm rss} = \left[\int h(t)^2\, dt\right]^{1/2} \tag{7}$$

which has units of $\sqrt{s}$ or $1/\sqrt{\rm Hz}$. In order to determine sensitivity, sine-gaussian waveforms are used, which are not unlike many expected astrophysical burst signals. The central frequency of each sine-gaussian is indicated in the figure. One curve labelled "LIGO-TAMA" is from a joint analysis using LIGO S2 and TAMA DT8 data. To get a feeling for the sensitivity, consider an isotropic GW source emitting a sine-gaussian waveform of frequency ≈ 150 Hz at 15 Mpc. This would correspond to a detection efficiency of 50% if about $0.2 M_\odot c^2$ of GW energy were released. For the S5 data, the

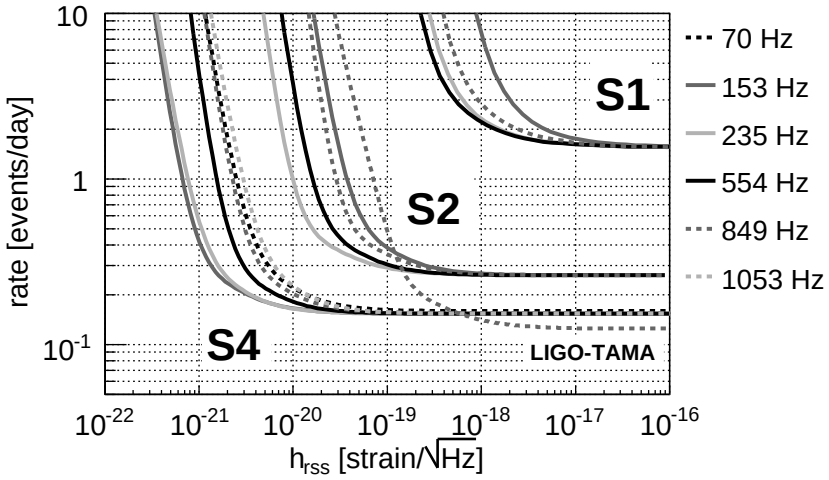

FIGURE 5. All sky 90% CL upper limit exclusion curves for GW bursts from the LIGO runs S1, S2, and S4. Each curve is for a signal at a particular frequency, represented by a sine-gaussian waveform. The excluded regions are above and to the right of each curve.

improved sensitivity would give, everything else being equal, about $0.05 M_\odot c^2$ of GW energy.

Gamma-ray Bursts

The standard model of gamma-ray burst (GRB) progenitors is that the long-duration (> 2 s) GRBs are associated with the core collapse of a massive star, while measurements in the last two years by the Swift mission[9] have bolstered the case for the association of short-duration GRBs with NS-BH (or NS-NS) mergers. In either case, one expects the emission of gravitational waves to be associated with the GRB events. The short GRBs are especially promising since compact mergers are expected to be efficient GW radiators and because these events are signifcantly less distant (redshift of ~ 0.4 compared to ~ 2.5 for long-duration GRBs), although the large distance for both classes of events means, in effect, that an unusually nearby GRB provides the best chance for a LIGO detection.

An analysis[10] of the S2, S3, and S4 data in association with 39 GRBs has been performed. Pairs of interferometer data are cross-correlated within 180 s of the GRB trigger ("on source" data segment) and compared with the identical cross-correlation analysis performed on a large number of data segments surrounding the on-source segment. The rather lengthy 180 s on source window takes into account the uncertainty associated with the detected GRB trigger time relative to the "true" GRB onset. No detections were observed. Figure 6 gives the 90% CL upper limits for $h_{\rm rss}$ (see Eq. 7) based on sine-gaussian waveforms with circular polarization at 250 Hz. For such a waveform, with measured sensitivity of $h_{\rm rss} = 10^{-21}$ Hz$^{-1/2}$, LIGO would be sensitive to the emission of $0.5 M_\odot c^2$ of GW energy at a distance of about 20 Mpc. For the first

17 months of the S5 run, there have been 157 GRB triggers. For 70% of these LIGO has had at least two interferometers in operation; about 25% have a measured redshift; and about 10% are short-duration GRBs.

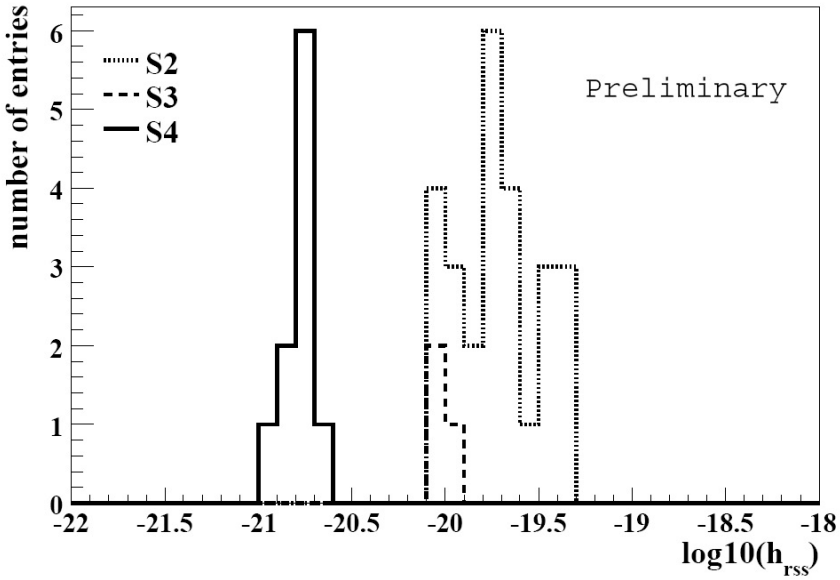

FIGURE 6. Preliminary 90% CL upper limits in $h_{\rm rss}$ for GW emission in association with GRB triggers in the S2, S3, and S4 science runs.

SGR analysis

Soft gamma-ray repeater (SGR) 1806-20 emitted a record flare on December 27, 2004. The pulsating tail of the flare lasted for 6 minutes. Some models predict that such oscillations are mechanically driven, and hence are potential GW sources. A LIGO analysis[11] has searched for excess power due to narrow-band signals of tens of seconds duration, following the same pattern as the observed electromagnetic oscillations. No significant excess was observed. For the 92.5 Hz quasi-periodic oscillation, the LIGO 90% CL upper limit corresponds to an isotropic energy release of $4.3 \times 10^{-8} M_{\odot} c^2$, which is comparable to the electromagnetic energy emitted by the flare. For this flare, LIGO was between science runs, but the H1 interferometer was operating. Future such analyses should benefit from better sensitivity as well as the power of correlating data between multiple interferometers.

PROSPECTS

Enhanced LIGO and Advanced LIGO

Following the end of the S5 run in fall 2007, a program called Enhanced LIGO will be initiated with the goal of improving sensitivity by about a factor of two. The

improvements are based in part on what has been learned from operating initial LIGO. Materials costs will be minor, and some technical improvements foreseen for Advanced LIGO will be included and tested, such as DC readout of the dark port photodiodes (rather than by RF modulation, as for initial LIGO). The installation schedule is about 18 months, after which an S6 science run is anticipated.

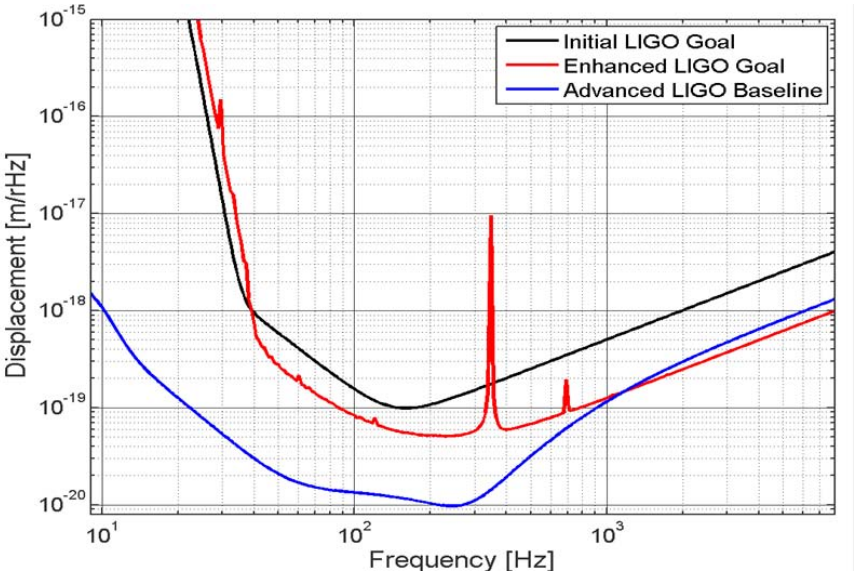

FIGURE 7. LIGO sensitivity curves in displacement (units of m per square root Hz). Shown is the initial LIGO goal, as also shown in Fig. 1, and the goals for Enhanced and Advanced LIGO. (Divide these curves by $L = 4000$ m to compare with the strain noise curves in Fig. 1.

Advanced LIGO[12] is a major upgrade program which will utilize the existing vacuum systems, but otherwise will replace or modify all other major systems. Prospects for initial funding of the project in the next year are promising. The sensitivity goal for Advanced LIGO is a factor 10 improvement relative to initial LIGO. Given large-scale strucure, this is expected to increase the number of GW sources by a factor of about $10^{2.7}$. In this case, even the most pessimistic estimates for the rate of compact binary coalescences would be accessible. The installation is planned to begin in late 2010, following S6, with science data to start in early 2014. The estimated sensitivity curves for the Enhanced and Advanced upgrades are shown in Fig, 7.

Toward a Global Network of GW Detectors

As mentioned earlier, the members of the GEO600 collaboration joined the LIGO Science Collaboration (LSC) early in the LIGO science running. Where appropriate, LSC analyses have included the GEO data. In January 2007, the LSC and the Virgo Collaboration[13] reached an agreement to share data and jointly analyze data. Virgo is a 3 km baseline interferometer which is designed to have a sensitivity similar to the 4 km LIGO instruments. A global network of interferometers will improve the sky coverage and sensitivity of future GW searches, and is clearly of great scientific benefit.

ACKNOWLEDGMENTS

The authors gratefully acknowledge the support of the United States National Science Foundation for the construction and operation of the LIGO Laboratory and the Particle Physics and Astronomy Research Council of the United Kingdom, the Max-Planck-Society and the State of Niedersachsen/Germany for support of the construction and operation of the GEO600 detector. The authors also gratefully acknowledge the support of the research by these agencies and by the Australian Research Council, the Natural Sciences and Engineering Research Council of Canada, the Council of Scientific and Industrial Research of India, the Department of Science and Technology of India, the Spanish Ministerio de Educacion y Ciencia, The National Aeronautics and Space Administration, the John Simon Guggenheim Foundation, the Alexander von Humboldt Foundation, the Leverhulme Trust, the David and Lucile Packard Foundation, the Research Corporation, and the Alfred P. Sloan Foundation.

REFERENCES

1. A. Abramovici, et al., *Science* **256**, 325–333 (1992).
2. K. S. Thorne, "Gravitational Radiation," in *300 Years of Gravitation*, 1987, pp. 330–457.
3. F. Pretorius, *Phys. Rev. Lett.* **95**, 121101 (2005).
4. B. Abbott, et al., *Nucl. Instrum. Meth.* **A517**, 154–179 (2004).
5. B. Abbott, *submitted to Phys. Rev. D* (2007), `gr-qc/07043368`.
6. B. Abbott, et al., *Astrophys. J.* **659**, 918–930 (2007).
7. B. Abbott, et al., *to appear in Phys. Rev. D* (2007), `gr-qc/0702039`.
8. B. Abbott, et al., *submitted to Class. Quant. Grav.* (2007), `gr-qc/07040943`.
9. N. Gehrels, et al., *Astrophys. J.* **611**, 1005 (2004).
10. B. Abbott, et al., Search for gravitational waves associated with 39 gamma-ray bursts using data from the second, third, and fourth ligo runs (2007), in preparation.
11. B. Abbott, et al., *submitted to Phys. Rev. D* (2007), `astro-ph/0703419`.
12. http://www.ligo.caltech.edu/advLIGO/ (2007).
13. F. Acernese, et al., *Class. Quant. Grav.* **23**, S635–S642 (2006).